A model of the transverse modes of stable and unstable porro−prism resonators using symmetry considerations

Liesl Burger[a,b †] and Andrew Forbes[a,b]
[a] CSIR National Laser Centre, PO Box 395, Pretoria 0001, South Africa
[b] School of Physics, University of Kwazulu−Natal, Private Bag X54001, Durban 4000, South Africa

ABSTRACT

A simple model of a Porro prism laser resonator has been found to correctly predict the formation of the "petal" mode patterns typical of these resonators. A geometrical analysis of the petals suggests that these petals are the lowest−order modes of this type of resonator. Further use of the model reveals the formation of more complex beam patterns, and the nature of these patterns is investigated. Also, the output of stable and unstable resonator modes is presented.

Keywords: Porro prism, laser resonator, petal patterns

1. INTRODUCTION

Porro prism lasers have the useful property of being insensitive to misalignment, making them rugged and suitable for field use. A tilt on a mirror deflects an incident beam by twice the tilt angle, whereas a tilt on a Porro prism has the effect of shifting the beam parallel to the axis of the incident beam. It is this property that makes these resonators insensitive to misalignment. Because of this they have been extensively used for many years in applications such as range−finding and target designation. Nevertheless, the resonator properties are not well understood.

Anan'ev[1] mentions the possibility that the finite bevels at the prism apexes explain the tendency for independent oscillation in different longitudinal sectors of the resonator, but does not go on to develop this idea into a model which explains experimental results. Recently[2,3] we have applied a physical optics approach to the Porro prism resonator which correctly predicts the salient features of the transverse modal patterns observed experimentally. With this model we are able to relate the properties of the laser beam to the mode patterns observed from such resonators. The model takes account of the losses on the apex of the prism, as well as the symmetry of the resonator.

Referring to Figure 1: When the resonator is viewed end−on the apexes of the prisms in the diagram are at an angle relative to each other, which is referred to as the Porro angle. (In the figure the Porro angle is drawn at 90°, the crossed−Porro configuration). The prisms can however be rotated to any angle with respect to each other. The effect of the prisms on the intracavity polarization in combination with the quarter−wave plate and beam−splitter cube results in the amount of radiation coupled out of the resonator being directly affected by the Porro angle. The Porro angle however also has an effect on the mode structure of the output beam.

If one considers an initial random low−intensity electromagnetic field (field (1) in Figure 1) travelling along the optical axis from Porro A to Porro B, it is simply cut off by the aperture in front of Porro A. The field will be reflected about the axis on the apex of Porro B and travel back along the optical axis, but the intensity distribution will show a decrease in a narrow rectangular area corresponding to the losses caused by the bevel on the apex of Porro B (field(2)). In a similar way, the subsequent reflection from Porro A (field (3)) will have a lower intensity in the area corresponding to the losses at the apex of Porro A. In this way, with the combined effects of loss at the apertures as well as on the prism apexes and the gain from the active medium, when the loss pattern repeats on the field a distinctive "petal" mode pattern is built up over a number of passes − 4 petals in the crossed−Porro case. In a similar way a 6−spot pattern develops when the prisms are 60° to each other, with 12 spots at 30°, with a complete description given in [3].

† Corresponding author: Liesl Burger; tel: +27 12 841 4207; fax: +27 12 841 3152; email: lburger1@csir.co.za

Laser Beam Shaping VIII, edited by Fred M. Dickey, David L. Shealy,
Proc. of SPIE Vol. 6663, 666305, (2007)
0277-786X/07/$18 · doi: 10.1117/12.734650

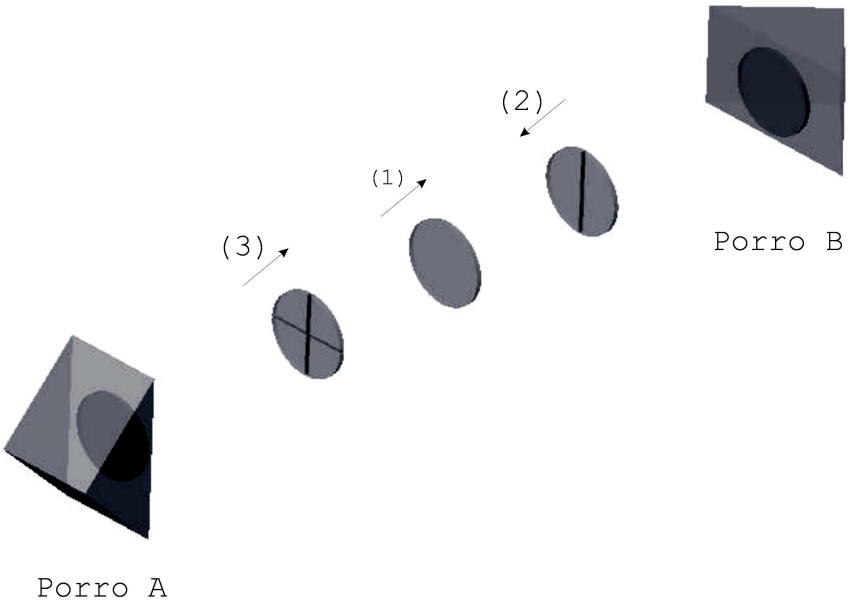

Figure 1: Formation of petal−pattern output beam.

The symmetry− and loss−analysis leads to a simple relationship between the Porro angle and the number of spots in the beam, and also implies that only an integral number of spots will develop a repetitive pattern[2].

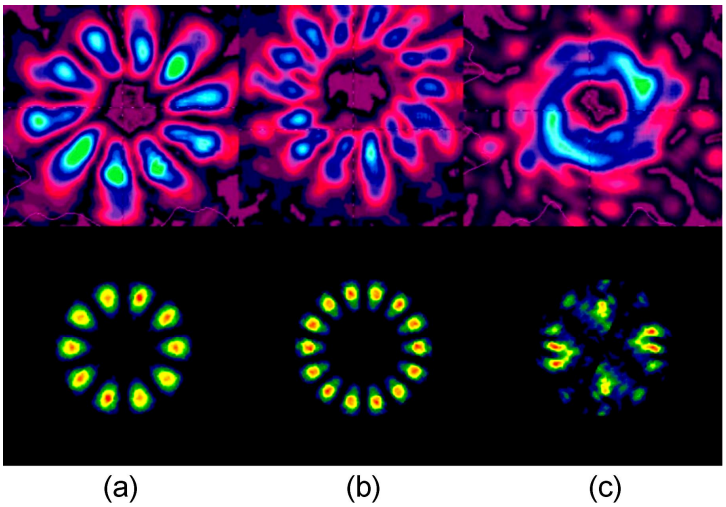

Figure 2: Petal pattern beam pattern (top) from experiment and (bottom) from the numerical model, with Porro angles (a) 36°, (b) 26° and (c) 50°.

Figure 2 (top row) shows the experimental images from an Nd:YAG Porro laser with Porro angles 36°, 26° and 50° respectively, as well as (bottom row) the beam pattern output by a numerical model of the identical resonator using the same Porro angles. It can clearly be seen that the Porro angles of 36° and 26° produce a petal mode pattern with 10 and 14 spots respectively, whereas the 50° case does not produce a temporally stable mode pattern.

In this paper an improved numerical model is presented, which was used to compare the resonator outputs for stable and unstable configurations. In Section 3 the model was used to probe the development of the output beam. The main finding was that the well−known petal mode is a special case and corresponds to the lowest−order mode of the system.

Section 4 describes an alternate configuration, and shows that on deeper investigation the mode structure of Porro resonator beams is far more complex.

2. SYSTEM DESCRIPTION

Figure 3 is a diagram of a typical Porro−prism laser. Porro prisms (components (a) in Figure 3) replace the traditional end mirrors in this simple straight resonator. The active medium, a cylindrical Neodymium−YAG rod (component (b)) is pumped by flashlamps. The laser is pulsed by a Cr^{4+}:YAG Q−switch or saturable absorber (component (c)). The use of the prisms precludes the use of a partially transmitting mirror to couple the radiation out of the resonator, so output coupling is done by polarization discrimination using a ¼−wave plate (component (d)) and a beam−splitter cube (component (e)). The stability of the resonator is determined by two lenses (components (f)) close to the prisms. These lenses allow the stability of the resonator to be determined using the stability parameters g_1 and g_2 of simple curved mirrors R_1 and R_2, where $g_1 = 1 - L/R_1$, $g_2 = 1 - L/R_2$. For simplicity identical lenses were used, making all of the resonators modelled symmetrical. Also shown are the limiting apertures (components (g)) in front of each prism. The specific resonator modelled had a length of L = 10 cm and the focal length of the intracavity lenses were varied to investigate beams obtained from different symmetrical resonators.

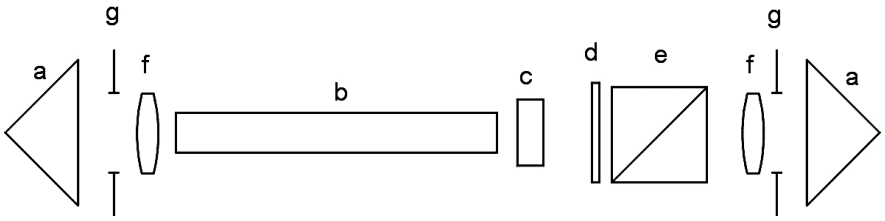

Figure 3: Diagram of Nd:YAG Porro prism laser resonator. (a) Porro prisms (b) active medium (c) Q−switch (d) 1/4−wave plate (e) beam−splitter cube (f) intracavity lenses (g) apertures.

The numerical model incorporates the following components, as labeled in Figure 3: prisms (a), the apertures (g), and the lenses (f), but does not model polarization and the effects of the ¼−wave plate (d) and beam−splitter cube (e), or the Q−switch (c). The gain is not modelled explicitly, but the beam energy is normalized on each pass to simulate this.

By keeping the resonator length fixed at 10 cm and by changing the values of the intracavity lenses a range of symmetrical stable and unstable resonators configurations were modelled. It was only possible to obtain the petal modes as well as the more complex modes from stable and marginally stable resonator configurations. In commercial Porro−prism lasers the most commonly used configuration is the flat−flat case (with no intracavity lenses), and the petal mode pattern is often reported experimentally and in the literature from this configuration. It was not possible to obtain any repeatable mode pattern from an unstable configuration. The reason for this is presumably because the beam needs to be contained for a large number of passes before a pattern can be established a condition which is only met in the stable case.

3. LOW−ORDER MODES

A number of resonators produce the above petal patterns in Figure 2. The following discussion uses by example a resonator which produces a petal patterns with 10 spots (corresponding to a Porro angle of 36°); it has a resonator length of 10 cm, no intracavity lenses (in other words a marginally stable resonator), and an intracavity aperture radius of 0.2 cm, corresponding to a Fresnel number of 37.59.

3.1 Temporal behavior of beam parameters

In order to investigate the development of these petal mode patterns the intensity, spot size, and loss were recorded after each round trip. A plot of these parameters shows how they develop with time, from switch−on and until the pattern stabilizes.

Figure 4(a) shows a plot of the losses as a function of the number of round trips completed by a field in the resonator. For the first few round−trips, when the field is essentially random noise and before a mode pattern emerges, the losses are very high and increase with the cumulative effect of the Porro apex losses on the field, as described in Section 1. Values between 6% and 9% are obtained as the mode develops in time, dropping to 3.3% as the mode collapses to fill the

available volume after approximately 300 round trips. The mode then remains constant in a low−loss region with round−trip losses of 3.3%.

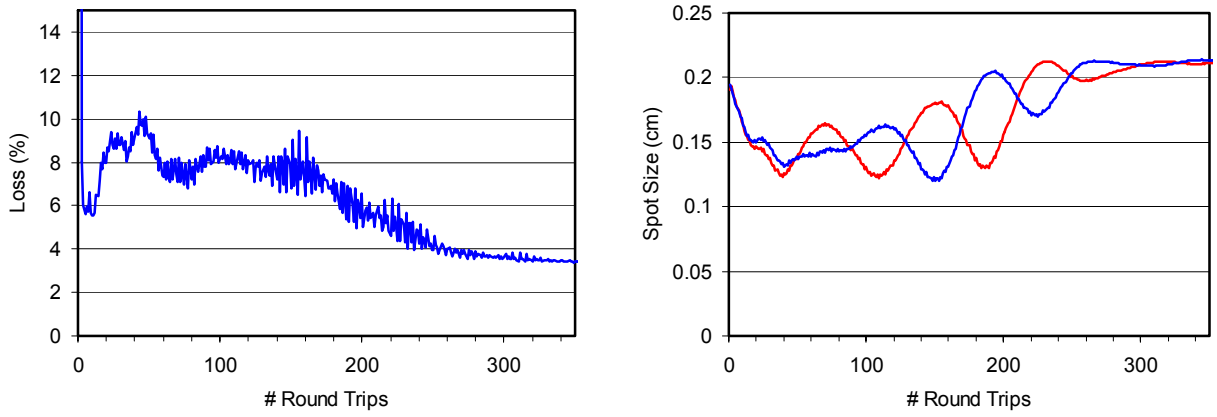

(a) (b)

Figure 4: Plot of (a) Loss and (b) Spot Sizes in the x− (blue) and y− (red) directions as a function of the number of round trips. Porro angle 36°, no intracavity lenses i.e. a marginally stable resonator.

Figure 4(b) shows the second−moment calculation of the output spot size (*not* the petal size) in the x− and y− directions as a function of the number of round−trips. There is an initial period of oscillation corresponding to competition between the modes, after which the spot size can be seen to stabilize to values of 0.21cm on both x− and y−directions. The emergence of the distinctive petal pattern coincides with the stabilization of the loss and spot size at about 300 round trips. An example of the output beam intensity is shown in Figure 2(a).

3.2 Petals are Gaussian−like

The output mode petal patterns obtained from this model (described in Section 2.1 above and show in Figure 2(a)) are stable with time, and symmetric. The petals are essentially circular in shape, with the highest intensities in the central region of each petal, each pattern reminiscent of a small Gaussian beam.

Following from the model of the petal−pattern formation[2,3] it is hypothesized that the petals are individual Gaussian−like modes, each resonating in the volume between both prisms in the cross−sectional area bordered by the Porro apexes as well as the circular limiting aperture. This is illustrated in Figure 5.

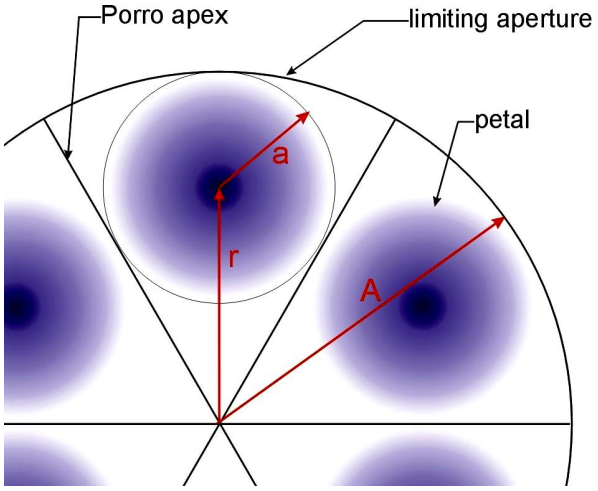

Figure 5: Diagram of Porro resonator viewed end−on, showing position and size of "Gaussian−like" petals.

The following analytical expressions for the position and size of a petal in the beam pattern are derived from the geometry of the largest circular area that can fit within each isolated loss−bounded area at a Porro prism. The criterion for minimal loss of a Gaussian beam passing through a circular aperture is used to predict the *petal* size: $a = 3\omega$, where a is the *petal* aperture radius, and ω is the *petal* spot radius.

The largest Gaussian that can fit inside this area is then calculated from simple geometry, and given by (1). The same geometrical analysis predicts the radial position of the petals in the output beam, and is given by (2).

$$\omega(A,n) = \frac{A}{3}\left(\frac{\sin\left(\frac{\pi}{n}\right)}{1+\sin\left(\frac{\pi}{n}\right)}\right), \tag{1}$$

$$r(A,n) = \frac{A}{1+\sin\left(\frac{\pi}{n}\right)}. \tag{2}$$

If each petal is Gaussian−like and a function of available space then these expressions for the petal size (ω) and position (r) in terms of the limiting aperture (A) and the number of spots (n) should hold.

By keeping the Porro angle fixed at 45° but varying the intracavity lenses and the limiting apertures in several of the numerical models the sizes of the petals (ω) of the output beams were estimated. These are plotted as data points, together with the analytical expression (given by Eq. (1)) for the petal size as a function of the limiting aperture radius A in Figure 6. The good agreement between the analytical expression and the measured data points supports the hypothesis that the petals which make up the output beam of a subset of Porro prism resonators can be though of as small Gaussian beams, each occupying its own radial sector but entire length of the resonator.

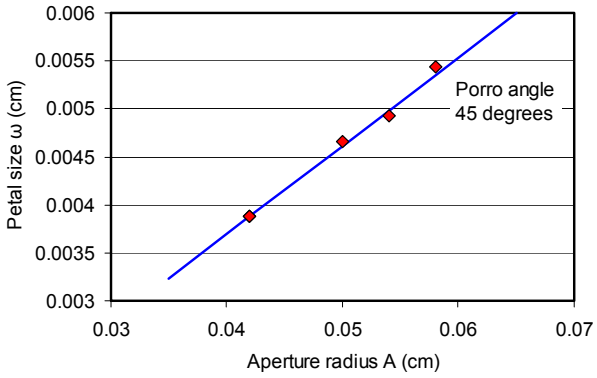

Figure 6: Plot of petal size as a function of aperture radius for a Porro angle of 45°. The line is a plot of the analytical function, and the points are measurements from the numerical model.

3.3 Far−field

When the petal−pattern output beam from the numerical model was propagated to the far−field the same petal pattern was observed. This unexpected result was generated by numerically propagating the beam to the far−field (using the criterion for the far−field of $\frac{A^2}{d\lambda} >> 1$, where d is the propagation distance), and also tested by propagating the output beam through a lens and thereby obtaining the Fourier transform of the beam in the focal plane. Both approaches showed the same result, shown in Figure 7.

This persistence of the mode pattern is a property of the fundamental modes of circular resonators, and further supports the hypothesis that the petals are small Gaussian−like beams, each appearing to resonate independently.

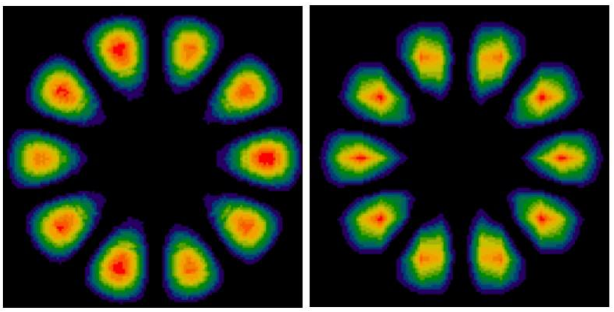

Figure 7: Near− and far−field modes (left and right respectively) from a Porro resonator with Porro angle 36°.

4. HIGHER−ORDER MODES

A number of different resonators were modelled using the same numerical model by changing the focal lengths of the intracavity lenses as well as the size of the intracavity apertures. Both intracavity lenses as well as both intracavity apertures were identical, making the resonator symmetric. When the apertures were increased beyond the region where petal patterns were observed an interesting output beam pattern became apparent to a greater or lesser extent. The following discussion will focus on the resonator with Porro angle of 30°, $g_1 = g_2 = 0.75$ and relatively large aperture A = 0.1 cm corresponding to a Fresnel number of 9.40, which best illustrates the effects noted.

4.1 Temporal behavior of beam parameters

Plots of the temporal behavior of the beam parameters provide some insight into the formation of the final beam structure. Initially the field is random noise, which has high losses, but the losses decrease steadily and rapidly; within 100 passes the losses have dropped to approximately 1% and stabilized to with 0.5%. Note that the losses in this resonator are significantly less than the final losses obtained for the petal−pattern case (3.3%) in Section 2.1 above.

A most interesting feature of this data is that a plot of the second−moment calculation of the spot size with time (Figure 8(b)) does not stabilize as expected (compare to Figure 4(b) above) but appears to oscillate.

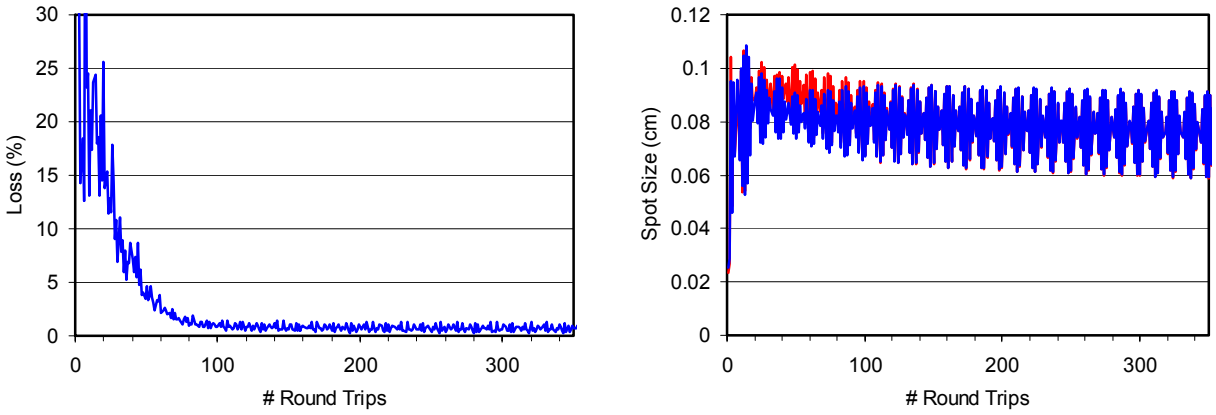

(a) (b)

Figure 8: Plots of the beam parameters (a) Loss, (b) Spot Size in the x− (blue) and y− (red) directions, (c) M^2 in the x− (blue) and y− (red) directions, all as a function of the number of round trips. Resonator has Porro angle 30°, $g_1 = g_2 = 0.75$, A = 0.1 cm.

Figure 9 is a detailed and expanded plot of the spot size data in Figure 8b, showing the period after 450 round trips. This scale reveals that there is indeed a pass−to−pass modulated oscillatory pattern to the spot size with time. The periodicity is 13 round−trips long in this case.

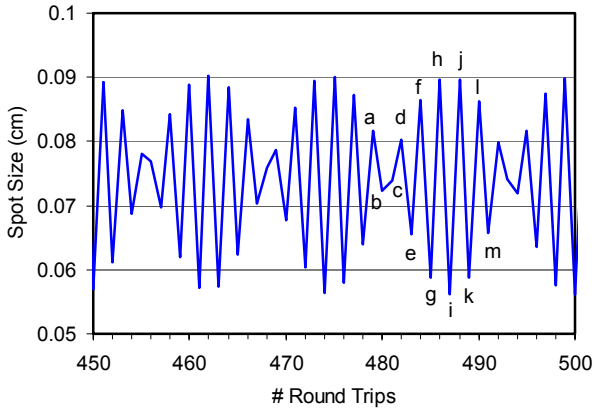

Figure 9: Detail of plot of Spot Size (x− and y−direction identical) from Figure 8(b).

The reason for this periodicity is evident when the mode patterns corresponding to the specific round trips in question (Figure 9 (a) to (m)) are examined. The mode patterns change on each round trip through the sequence of 13 round trips as shown in the mode patterns (a) to (m) in Figure 10, and then this series cycles over and over, never appearing to stabilize to a static mode pattern as did the petal pattern in Section 2.1 above.

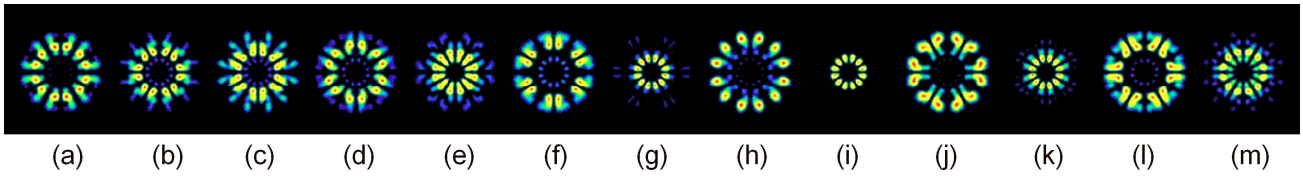

Figure 10: Repeating sequence of 13 output modes, Porro angle 30°, $g_1 = g_2 = 0.75$, $A = 0.1$ cm.

The mode patterns in Figure 10 will not be observed directly when an attempt is made to verify the model experimentally, because the mode patterns follow each other by the time taken for light to travel just one round trip, and too short to be captured by a camera. Rather it is expected that a time−average of these modes will be visible.

If the petal mode is the lowest−order mode of the Porro−prism resonator, analogous to the Gaussian mode of circular resonators, then it is reasonable to extend the hypothesis and suppose that the mode patterns shown in Figure 10 are (or are combinations of) the higher−order modes of these resonators, and analogous to the Laguerre−Gaussian modes of circular resonators.

5. CONCLUSION

A numerical model of a Porro prism resonator was written that correctly predicts the formation of a petal pattern output beam. It was possible to produce a beam pattern only for the stable resonator configurations modelled, but not for the unstable configurations. The mode pattern, round−trip loss, M^2 and output spot size were recorded until the beam stabilized, and helped to explain the formation of the final mode patterns. The simple petal beam structure appears to be the lowest−order fundamental mode of the Porro prism resonator analogous to the circular resonator's Gaussian mode. Higher−order modes show a cyclic repetition of modes, and could be combinations of the higher−order modes of this type of resonator. Current and future work will be directed towards modeling the gain and Q−switch, as well as towards finding an explanation for the more complex beam structure observed in resonators with larger apertures than those producing the petal patterns. An attempt will also be made to verify the complex modes experimentally.

REFERENCES

1. T.A. Anan'ev, "Unstable prism resonators," *Sov. J. Quant. Electron.,* 3(1), 58–59 (1973).
2. I.A. Litvin, L. Burger, A. Forbes, "Analysis of transverse field distributions in Porro prism resonators", *Proc. SPIE* Vol. 6346, 63462G-1 − 63462G-7 (2007).
3. A. Forbes, L. Burger and I.A. Litvin, "Modelling laser brightness from cross Porro prism resonators," *Proc. SPIE* Vol. 6290, 62900M-1 − 62900M-8 (2006).